DRAFT VERSION MAY 17, 2013
Preprint typeset using LaTeX style emulateapj v. 11/12/01

USING MEGAMASER DISKS TO PROBE BLACK HOLE ACCRETION

JENNY E. GREENE[1,8], ANIL SETH[2], MARK DEN BROK[2], JAMES A. BRAATZ[3], CHRISTIAN HENKEL[4,9], AI-LEI SUN[1], CHIEN Y. PENG[5], CHENG-YU KUO[6], C. M. VIOLETTE IMPELLIZZERI[3,7], K. Y. LO [3]

Draft version May 17, 2013

ABSTRACT

We examine the alignment between H_2O megamaser disks on sub-pc scales with circumnuclear disks and bars on < 500 pc scales observed with *HST*/WFC3. The *HST* imaging reveals young stars, indicating the presence of gas. The megamaser disks are not well aligned with the circumnuclear bars or disks as traced by stars in the *HST* images. We speculate on the implications of the observed misalignments for fueling supermassive black holes in gas-rich spiral galaxies. In contrast, we find a strong preference for the rotation axes of the megamaser disks to align with radio continuum jets observed on $\gtrsim 50$ pc scales, in those galaxies for which radio continuum detections are available. Sub-arcsecond observations of molecular gas with ALMA will enable a more complete understanding of the interplay between circumnuclear structures.

1. INTRODUCTION

Active galactic nuclei have always posed a basic and fundamental problem – how to cram gas that is happily rotating on kpc scales onto an accretion disk on AU scales (e.g., Balick & Heckman 1982). We do not know the mechanism that dissipates angular momentum and allows gas to accrete. There are no shortage of ideas, including major or minor mergers (e.g., Sanders et al. 1988; Hopkins et al. 2006), bars or bars within bars (e.g., Shlosman et al. 1990; Maciejewski et al. 2002; Hunt et al. 2008; Kim et al. 2012), or nuclear spirals (Englmaier & Shlosman 2000; Maciejewski 2004; Martini et al. 2003; Ann & Thakur 2005). In a couple of nearby cases, inflows are directly observed along circumnuclear spirals in ionized gas on hundreds of pc scales (e.g., Storchi-Bergmann et al. 2007; Davies et al. 2009).

One intriguing clue to the origin of accreting gas comes from the well-known misalignment between the rotation axes of accretion disks and the galaxy-scale disk, typically measured using radio jets as a tracer of the angular momentum on sub-pc scales (e.g., Ulvestad & Wilson 1984). In this paper we use 22 GHz water megamaser emission as a tracer of sub-pc–scale accretion disks (e.g., Miyoshi et al. 1995; Lo 2005). Early examples of megamaser disks revealed the same misalignment, this time between the outer galaxy disk and the ~ 0.5 pc molecular disk producing the masers (e.g., Braatz et al. 1997; Greenhill et al. 2009). The interpretation is ambiguous. Perhaps the galaxy swallowed some small gas-rich galaxy that is providing fuel with a random orientation, or perhaps the accretion process involves torques in which angular momentum is not conserved as a function of scale.

The sample of megamaser disk galaxies mapped with Very Long Baseline Interferometry has grown considerably in the past few years (e.g., Reid et al. 2009; Kuo et al. 2011), and the trend of misalignment continues. Here, we contribute *Hubble Space Telescope* observations of nine megamaser host galaxies. Combining *HST*/WFC3 imaging from F336W to F160W, we are able to identify disk-like structures on $\lesssim 500$ pc scales in the majority of the sample galaxies. Even on these circumnuclear scales, we find no evidence for alignment with the megamaser disks.

2. CIRCUMNUCLEAR STRUCTURES

We observed nine megamaser disk galaxies with *HST* in Cycle 18 under GO-12185. We have examined the $M_{\rm BH}-\sigma_*$ relation of these galaxies already (Greene et al. 2010), and proposed to study the correlations between galaxy bulge properties and $M_{\rm BH}$ with *HST*. The galaxies are all $\sim L^*$ spirals with $M_B \approx 21$ mag and Hubble types ranging from S0 to Sbc (Greene et al. 2010). In two orbits, we obtained F336W, F438W, F814W, F110W, and F160W (roughly *UBIJH*) images of each galaxy with integration times of $1320, 430, 2140, 150, 420$ sec respectively. Two galaxies (NGC 6264 and NGC 6323) are more distant than 100 Mpc, which prohibits the analysis presented here. Thus we limit our attention to the seven nearest galaxies in our sample (Table 1), including five galaxies from Kuo et al. (2011), NGC 3393 (Kondratko et al. 2008), and IC 2560 (Ishihara et al. 2001). Published VLBI maps reveal the orientation of the masing disk very precisely in all cases but IC 2560, where we rely on unpublished information (Wagner et al. in prep). We follow the convention of Kuo et al. and refer to the position angle (PA) of the megamaser disk as the angle East of North to the blue-shifted side of the disk.

2.1. *Identifying circumnuclear structures*

We use a combination of ellipse-fitting and color maps to identify organized circumnuclear structures such as nuclear bars (e.g., Maciejewski et al. 2002; Erwin & Sparke 2003), nuclear rings (e.g., Buta 1986), or nuclear spirals (e.g., Martini et al. 2003). The ellipse fits are performed on the F160W

[1] Department of Astrophysics, Princeton University, Princeton, NJ 08540
[2] University of Utah, Salt Lake City, UT 84112
[3] National Radio Astronomy Observatory, 520 Edgemont Road, Charlottesville, VA 22903, USA
[4] Max-Planck-Institut für Radioastronomie, Auf dem Hügel 69, 53121 Bonn, Germany
[5] GMTO Corporation. 251 S. Lake Ave., Suite 300. Pasadena, C 91101
[6] ASIAA
[7] Joint Alma Office, Alsonso de Cordova 3107, Vitacura, Santiago, Chile
[8] Alfred P. Sloan Fellow
[9] Astron. Dept., Kind Abdulaziz University, P.O. 80203, Jeddah, Saudi Arabia

Table 1. Megamaser Galaxies

Galaxy (1)	D (2)	HT (3)	Diam (4)	P.A. (5)	$\mathrm{Diam_{CN}}$ (6)	$\mathrm{P.A._{CN}}$ (7)	$\mathrm{Diam_{maser}}$ (8)	$\mathrm{P.A._{maser}}$ (9)	S_{Jet} (10)	λ_{Jet} (11)	L_{Jet} (12)	$\mathrm{PA_{Jet}}$ (13)	$\mathrm{Ref_{Jet}}$ (14)
NGC1194	52	SA0	24	143	···	150	1.3	160	0.6	3.6	70	56	1
NGC2273	26	SB(r)a:	24	62	0.25	30	0.1	150	19	6	170	90	2
UGC3789	50	(R)SA(r)ab	23	152	0.73	180	0.3	40	14.4	20	2900	145	FIRST
NGC2960	71	S0a	37	48	1.0	50	0.4	−130	1.6	20	7000	145	3
IC2560	42	(R')SB(r)b	32	45	0.40	40	0.3	135	···	···	···	···	···
NGC3393	53	(R')SB(rs)	34	161	0.52	150	0.4	−30	13	3.6	680	56	1
NGC4388	19	SA(s)b:	26	90	···	90	0.3	110	190	3.6	···	24	4

Note. — Col. (1): Galaxy. Col. (2): Distance to the galaxy (Mpc) from Kuo et al. (2011). Col. (3): Hubble Type, as modified from NED based on our *HST* images. Col. (4): Galaxy diameter (kpc) from NED. Col. (5): Position angle of the galaxy as a whole measured E of N. These measurements have an uncertainty of $\sim 10^\circ$. Our measurements agree with those from NED to within 10° in all cases. Col. (6): Size (kpc) of circumnuclear disks or bars. Col. (7): Position angle of structure in Col. (6) E of N. Col. (8): Outer radius of the megamaser disks (pc), as measured by Kuo et al. (2012), except for NGC 3393 that was measured by Kondratko et al. (2008). Col. (9): Position angle of megamaser disk measured east of north. P.A. equals zero when the blueshifted side of the disk plane has zero east offset and positive north offset. Note that all megamaser disks except for NGC 4388 have a measured inclination $> 86^\circ$, and are thus effectively edge-on. All are published but IC 2560, where we rely on unpublished information (Wagner et al. in prep). Col. (10): The flux of a detected elongated radio structure (mJy). When there are multiple jet structures on different scales, we tabulate the most compact imaged jet. Col. (11): Wavelength of detected jet (cm). Col. (12): The extent of the radio jet (pc). Col. (13): Position angle (East of North) of the radio jet ($^\circ$). Col. (14): Source of the radio observations: (1) Schmitt et al. (2001) (2); Ulvestad & Wilson (1984); (3) A. Sun et al. in preparation; (4) Falcke et al. (1998); FIRST: Becker et al. (1994).

images using the algorithm of Jedrzejewski (1987) as implemented by the IRAF code `ellipse`. The code fits ellipses to the galaxy isophotes, allowing the center, position angle (PA), and ellipticity ($e = 1 - b/a$, where a, b are the major and minor axis respectively) to vary as a function of radius. Circumnuclear structures are identified based on peaks and valleys in ellipticity with corresponding changes in PA pointing to the presence of nuclear bars or spirals (e.g., Erwin & Sparke 2003). Color information provides secondary clues as to the nature of the structures that we identify. For instance, nuclear rings are identified as red or blue rings (e.g., Buta & Crocker 1993). Note that while we do not have direct observations of gas yet, blue colors that identify recent star formation identify gas-rich regions by inference. Our primary interest here is not in identifying all galactic structures. Instead, we are most interested in the projected PA of the circumnuclear ($\lesssim 500$ pc) structures, for comparison with the PA of the megamaser disks (Figure 1).

We must be careful in interpreting blue colors in the circumnuclear region, because the active galactic nuclei (AGNs) are exciting narrow-line region emission that also falls into our broad-band filters. We use a pixel-by-pixel fitting method to isolate pixels that are dominated in the blue by narrow emission lines. For each pixel in the three optical bands (F336W, F438W, F814W), we explore a grid of single stellar population (SSP) models (Bressan et al. 2012), with metallicities in the range [Fe/H]= −1 to 0 (although our results are not sensitive to the exact range of metallicity), and age running from 1 Myr to 13 Gyr. Each grid point produces two colors, effectively $U-B$ and $B-I$. Dust is present in almost all of our galaxies, but we are only interested in identifying emission-line gas. Thus we use, for each pixel and grid point, a range of extinction values ($\mathrm{A}_V = 0-50$) to modify the SSP colors according to a standard extinction law (Girardi et al. 2008). We then determine the maximum likelihood value for each pixel by comparing the likelihoods of all grid points and extinction values. We conservatively mask all pixels with a low maximum likelihood (corresponding to $\chi^2 > 4$). Note that we have not masked the F160W images in making our ellipticity profiles. There are emission lines in these bands, but their equivalent width is low. As an extreme example, the famous S-shaped emission region in NGC 3393 is detected weakly in the F160W image, but has no impact on the measured PA, which is nearly orthogonal to the orientation of the narrow-line region.

2.2. *Circumnuclear structures and megamaser disks*

In three galaxies (NGC 2273, NGC 2960 or Mrk 1419, and UGC 3789) we see evidence for a circumnuclear disk. In the case of NGC 2273 and UGC 3789, there is an inner ring which manifests as a spike in the ellipticity profile, and then dust-lanes interior to the ring most readily identified with spiral arms. In the case of NGC 2273, kinematic data confirm this interpretation (Barbosa et al. 2006; Falcón-Barroso et al. 2006). We find a blue structure in the inner $\sim 3''$ of NGC 2960 with constant PA and ellipticity as the outer disk. Within the inner $\sim 1''$, there is a PA change likely associated with the narrow-line region gas, as shown (Figure 1).

NGC 3393 also shows a bar and maybe a ring on $\sim 20''$ scales, and then has what appears to be a nuclear bar on $\sim 3''$ scales. At the position of the bar, we see an ellipticity maximum at a constant position angle, the classic signature of a bar (e.g., Wozniak et al. 1995; Menéndez-Delmestre et al. 2007). IC 2560 is a difficult case, because the central blue light is dominated by narrow-line emission. On kpc-scales ($> 30''$), the galaxy shows the classic signature of an X-shaped bar (e.g., Li et al. 2011). However, in the nucleus, dust obscuration and narrow-line emission conspire to make identification of any organized structure quite difficult. Since the PA profile is flat for radii $r > 0.5''$, we assign IC 2560 an inner PA of 45°, but caution that the identification in this case is uncertain. Finally, we have no information for NGC 4388 or NGC 1194, which are edge-on, such that dust from the galaxies on large scales obscures the nucleus. In these two cases we adopt the PA of the large-scale disk (Figure 2).

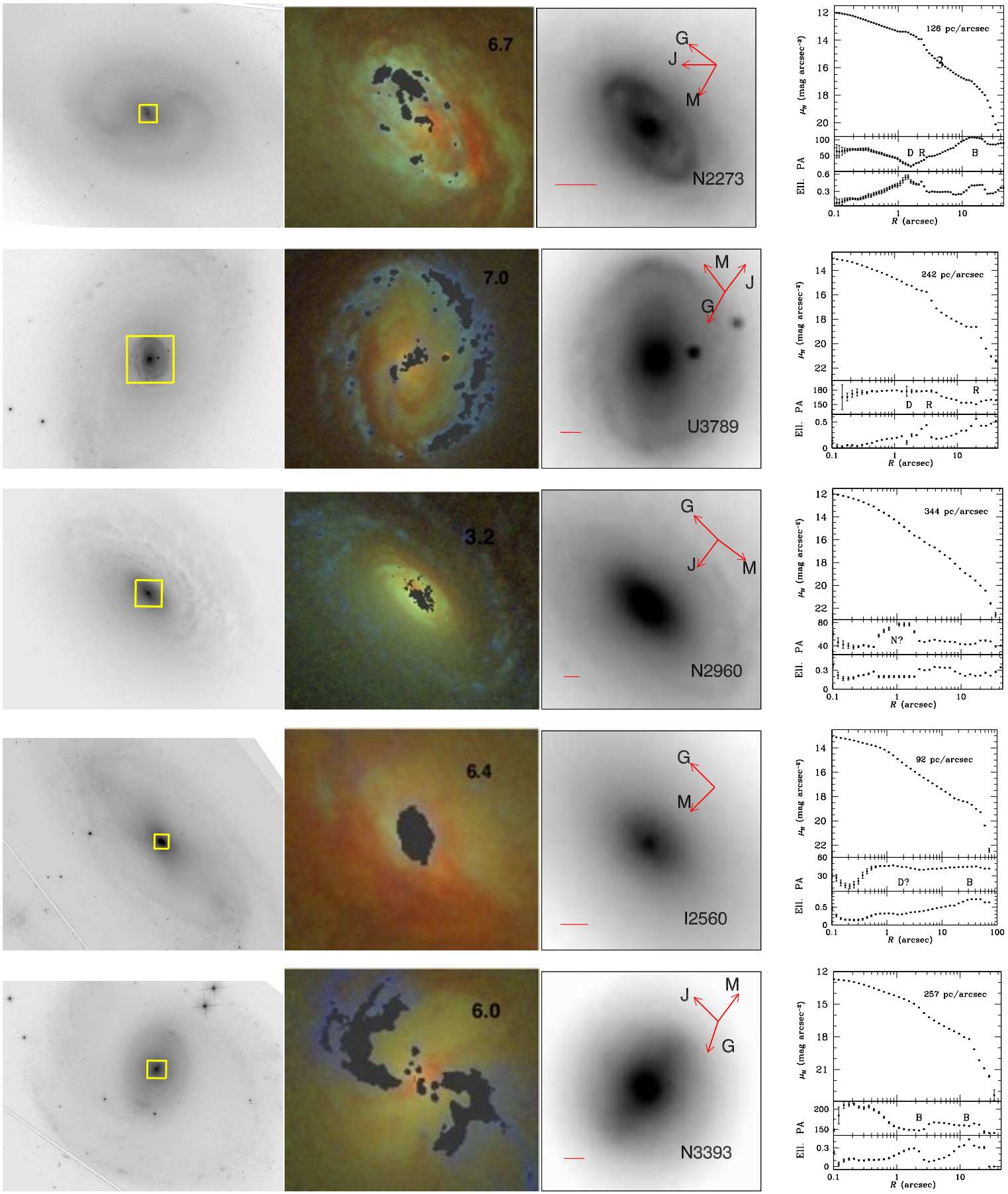

FIG. 1.— Images of the five megamaser disk galaxies from our *HST* program that appear to contain circumnuclear disks or bars on < 500 pc scales. North is up and East to the left. For each galaxy we show, from left to right, the F814W image on large scales, a three-color image made with F336W, F438W, and F814W, and the F160W image. The central and right-most images are shown on the same scale, as indicated by the yellow box in the left-most image. The angular scale (in arcsec) is indicated in the upper right of the color image, while the red scale bar in the right-most image indicates 200 pc. In the central three-color image, red light indicates both reddened regions and older stellar populations, while blue light indicates recent star formation. The grey regions are pixels that have been masked because the colors are dominated by narrow line emission rather than starlight. In the right-most F160W image the red arrows show the orientation of the kpc-scale galaxy (G), the megamaser disk (M) and a jet if known (J; see also Table 1). Recall that the megamaser disks are effectively edge-on in all cases, unlike the large-scale galaxies, and the arrow points towards the blue-shifted component of the disk. Finally, we show the radial profile from *ellipse*, along with the radial distribution in ellipticity and PA. All identified structures are marked as B=bar, D=disk, N=narrow-line emission, and R=ring.

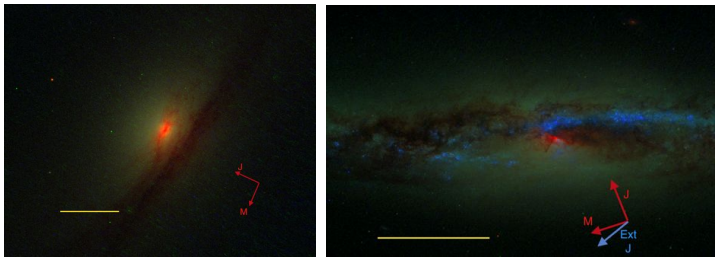

FIG. 2.— Three color images for the edge-on galaxies NGC 1194 (left) and NGC 4388 (right), constructed as above but without masking. The yellow scale bar indicates 1 kpc while the red arrows indicate the jet (J) and the direction towards the blue-shifted side of the megamaser disk (M). The blue arrow indicates the extended jet (Ext J) directions.

As an alternate way to look at the data, we also generate structure maps from the F814W images (Pogge & Martini 2002) shown in Figure 3. Structure maps use deconvolution to remove large-scale power and highlight fine structures from dust (dark in our maps) and emission-line regions excited either by the AGN or star formation (bright in the structure maps). These emphasize the dust structures in NGC 2273, NGC 2960, and IC 2560. There is dust structure apparent in UGC 3789, although it is subtle. However, the structure in NGC 3393 is dominated by the narrow-line region emission (see also the mask in Figure 1). In summary, for the five megamaser disk galaxies studied here, whose large-scale galaxies are not edge-on (Figure 1), we find clear evidence for circumnuclear disks or bars in four cases. We previously suggested that the majority of the megamaser disks are found in pseudobulge galaxies (Greene et al. 2010). Now, with the high spatial resolution of *HST*, we have confirmed that there is evidence for ongoing secular evolution in the circumnuclear regions of these galaxies, as expected for pseudobulges (e.g., Kormendy & Kennicutt 2004).

Having identified these circumnuclear structures, we now must assign a projected position angle to each. We use the PA from the ellipse fitting at the scale of the feature, often corresponding to a local extreme value in ellipticity. As described in Erwin & Sparke (2003), projection effects (e.g., the superposition of a bright bulge and a nuclear bar) can lead to offsets between the isophotes and the measured PA. However, based on visual inspection of our galaxies, we believe that our values are good to $\sim 10^\circ$. Table 1 contains the orientation and linear size of each circumnuclear structure. The nuclear disk in NGC 2273 (radius of $2''$ or 260 pc) is well-studied (Erwin & Sparke 2003), and our PA agrees with the literature value within our uncertainty of 10°. For the remainder of the paper, we will focus on comparisons between the PA of these circumnuclear structures on 100-500 pc scales with the megamaser disks on sub-pc scales. If we need to refer to larger scales in the galaxy, we will refer to the kpc-scale galaxy.

In principle, we are also interested in the distribution of inclinations for these circumnuclear structures. Taking the ellipticity measurements at the same radius as the PA measurements and assuming thin disks, we find that all of the targets have high inclinations ($i > 55^\circ$). However, it is not at all clear that we are identifying thin disks in all cases.

We show the distribution of $\Delta\mathrm{PA} \equiv \mathrm{PA_{disk}} - \mathrm{PA_{maser}}$ in Figure 4*a*. The first main result of this paper, highlighted in Figure 4*a*, is that the megamaser disks do not tend to align with the circumnuclear structures ($\lesssim 500$ pc) traced by *HST*. We have also included NGC 1068, Circinus, and NGC 3079, where the circumnuclear disk PA is measured from molecular disks. In the case of Circinus, the megamaser disk is warped, and we take the PA of the inner disk. The molecular disk in NGC 1068 is warped, but in inclination rather than in PA.

Of course, we are interested in the orientation of the stars and the gas. With the *HST* images, we infer the presence of gas based on either blue colors corresponding to recent star formation or dust lanes. We have neither gas or stellar kinematic observations at these sub-arcsecond scales yet. However, in the megamaser galaxies NGC 1068, NGC 3079, Circinus, and NGC 2273, detailed gas observations do exist. The detailed interpretation is different in each case. In NGC 1068, Schinnerer et al. (2000) probe ~ 20 pc scales with CO, and show that the molecular gas disk has a warp that starts at ~ 70 pc and extends all the way to the maser disk on 1 pc scales. NGC 3079 contains a kpc-scale molecular disk that is aligned with the major axis of the galaxy, and then a 600-pc scale molecular oval that is aligned in PA both with the kpc-scale disk and the pc-scale masing disk (Koda et al. 2002; Kondratko et al. 2005). In Circinus, the maser disk is nearly perpendicular to the bipolar radio jet and a CO outflow (Greenhill et al. 2003). Finally, the kinematic major and minor axes of the disk in NGC 2273 are not aligned, and the disk is likely warped (e.g., Barbosa et al. 2006). The CO disk appears to align with the warped disk on 200 pc scales (Petitpas & Wilson 2002), while the megamaser disk is misaligned in PA by 60°. Existing observations of gas and kinematics thus suggest that the circumnuclear structures observed here are manifestations of torques that facilitate accretion onto smaller scales.

In conclusion, for objects where $\lesssim$ 500pc-scale gas or stellar structure observations are available, 40% show a misalignment $\gtrsim 20^\circ$ with the masing disks. We see no tendency for alignment between the stellar structures traced by *HST* and the megamaser disks, although the gas structures do tend to align. Note that because we focus here on projected position angles, we are observing a lower limit on the misalignments.

3. NUCLEAR JET TO DISK ANGLE

We have seen that stellar structures on $\lesssim 500$ pc are frequently misaligned with the sub-pc scale accretion disk. We still expect that the nuclear jet should emerge along the rotation axis of the sub-pc scale disk (e.g., Pringle et al. 1999). Since the megamaser disks must be close to edge-on in order for amplification to occur, the jets should be perpendicular to the megamaser disk positions on the sky. Indeed, Henkel et al. (2005) found a high rate of megamaser detections in galaxies where the jet was likely in the plane of the sky, suggesting that jets are usually aligned with the rotation axis of the maser disk. We are able to observe the relative orientation of the megamaser disk rotation axis and the jet directly.

Most objects in our sample have been observed in the radio continuum at relatively high angular resolution (Table 1), including NGC 1194, NGC 3393 (Schmitt et al. 2001), NGC 2273 (Ulvestad & Wilson 1984), IC 2560 (Morganti et al. 1999), and NGC 4388 (Falcke et al. 1998). In the case of UGC 3789, we simply quote the FIRST fit on kpc scales since no higher resolution data are yet available. Finally, for NGC 2960 we measured a marginally resolved structure at 20 cm from our EVLA observations with a size of $20 \pm 3''$ (A. Sun et al. in preparation). Only IC 2560 is unresolved (on the $1''$ or 0.2 kpc scales measured by Morganti et al.). We caution that these observations probe jets on tens of pc scales and in some cases, VLBI observations do reveal PA changes on pc scales (e.g., Ul-

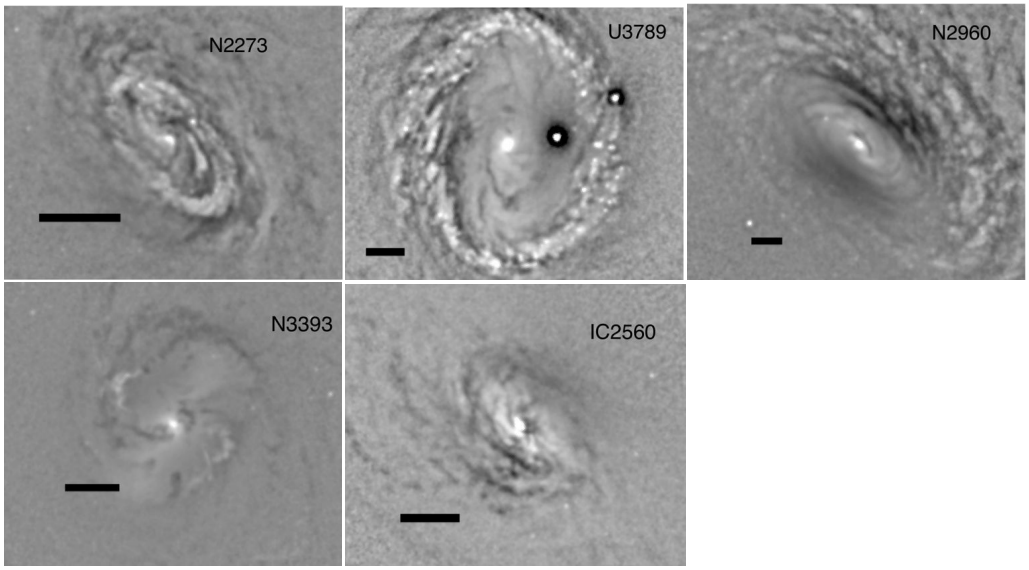

FIG. 3.— Structure maps (Pogge & Martini 2002) made in with F814W to emphasize the circumnuclear dust structure. Dark regions are dust lanes while bright regions correspond to emission line knots due to either star formation or narrow-line region gas. We have zoomed in on comparable regions as seen in the color maps in Figure 1, with the black scale bars again indicating 200 pc. In the case of NGC 2273, NGC 2960, and IC 2560, the dust structure is clear. UGC 3789 appears to show two arms reaching towards the center inside the inner ring. The structure in NGC 3393 is dominated by the narrow-line gas.

vestad et al. 1998; Middelberg et al. 2004). In fact, the pc-scale jet in NGC 3079 is misaligned (Trotter et al. 1998), while the diffuse radio emission on pc scales is aligned with the rotation axis of the disk (Duric & Seaquist 1988). Given the alignment that we report on tens of pc scales, it would be quite interesting to see different behavior on pc scales for more of our sources, in light of the possibility that the jet axis may be determined on small scales by the black hole spin but on large (tens of pc scales) by electromagnetric forces from the disk (McKinney et al. 2013).

In Figure 4*b*, we show the distribution of ΔPA for the projected jet and megamaser disk angles. Note that the megamaser disks are edge-on, so the PA is determined by measuring the angle on the sky of the observed linear alignment of maser spots and is 90° from the rotation axis of the disk. As Figure 4 shows, the vast majority of the jets are aligned with the rotation axis of the megamaser disk, as expected. We more than double the number of systems with a direct disk-jet comparison (Herrnstein et al. 1999; Greenhill et al. 2003; Kondratko et al. 2005). The largest outliers are are NGC 3079 (ΔPA= 44°) and NGC 2273 (ΔPA= 60°). In summary, in all but one of the systems, the jets on tens of pc to kpc scales are found to align within $< 15°$ of the megamaser rotation axis.

In addition to compact jets, we would eventually like to investigate possible kpc-scales jets to seek evidence of a change in direction of the accretion disk on longer timescales. For instance, radiation-pressure–driven warping may drive sub-pc scale disk precession on $\sim 10^6$ year timescales (e.g., Pringle 1997). Furthermore, it is interesting to ask whether ionization cones align with the jet/megamaser disk rotation axis. We do not really have complete information on the orientation of the narrow-line regions for the full sample. However, from the masked (grey) pixels in Figure 1, we can see that the spectacular S-shaped narrow-line region in NGC 3393 does align with the radio jet and the megamaser rotation axis (e.g., Cooke et al. 2000; Kondratko et al. 2008), and this is seen in Circinus as well (Greenhill et al. 2003). In other cases, we do not have adequate information yet to address the relative orientation of any ionization cones.

4. WARPS AND KINEMATIC MISALIGNMENTS FACILITATE ACCRETION

We have seen that nuclear (and in some cases extended) radio jets align with the rotation axis of the megamaser disks. In contrast, the sub-pc scale accretion disk does not align with the kpc-scale galactic disk (see §1). Using *HST*/WFC3 imaging, we have found no strong tendency for alignment between the megamaser disks and the circumnuclear structures traced by stars on $\lesssim 500$ pc scales. Here we review what these misalignments may tell us about the accretion process.

Disk warping on pc scales causes the observed misalignments. One route to disk misalignment is warping of the pc-scale accretion disk. According to Pringle (e.g., 1997), the sub-pc scale disk may change position angle by a significant fraction due to radiation pressure. For the megamaser disks, the typical timescale for disk PA changes due to radiation-pressure warping would be $\sim 5 \times 10^6$ yr (see also Maloney et al. 1996; Gammie et al. 2000) with only a linear dependence on BH mass. AGN lifetimes are very uncertain, but Martini et al. (2003) suggest that accretion episodes in low-luminosity sources may only last millions of years, perhaps just long enough for some PA change over the AGN lifetime. Note that radiation pressure warping cannot cause the warps observed on circumnuclear (~ 200 pc) scales in NGC 2273 and NGC 1068.

Another possible source of sub-pc–scale torques comes from stars in a cusp around the BH; Bregman & Alexander (2012) find that resonant relaxation with a stellar cusp will drive warping of order 10° on sub-pc scales, comparable to the warp in NGC 4258. The expected timescale for evolution is $\sim 10^7$ yr for NGC 4258, perhaps in some tension with the million-year lifetimes from Martini et al. Alternatively, Kartje et al. (1999) suggest that masing clumps are accelerated out of the disk plane by magnetic pressure to a height where the balance of shielding and pumping is optimal. Since the optimal height will depend on the AGN luminosity, they predict more warping at higher luminosities. Both radiation pressure and stellar resonance warping act on sub-pc scales, i.e. on the scales of the megamaser disks. Warping does not appear to be a compelling explanation in general for the observed misalignments for three reasons. First, in contrast to NGC 4258, the observed warps in the new megamaser disks are $< 10°$ (Impellizzeri et al. 2012; Reid et al. 2013; Kuo et al. 2013) and thus smaller than predicted by either warping model. Second, the observed warps are too small to explain the broad range of PA differences that we ob-

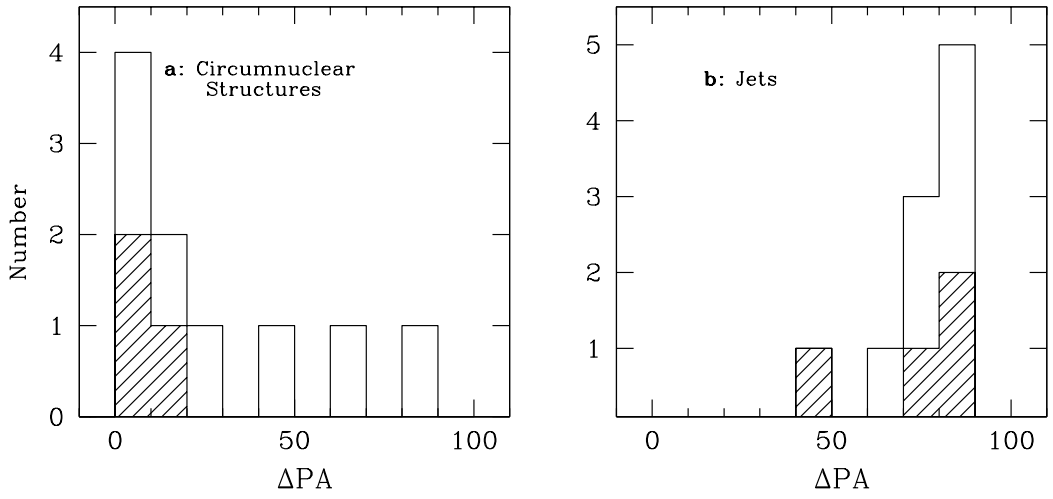

FIG. 4.— Histogram of the difference in projected position angle between the megamaser disk and (*left*): the circumnuclear structures on $\lesssim$500 pc scales identified in the *HST* images and (*right*): the most compact jet structure we could find in the literature, as summarized in Table 1 (note – this is the PA of the megamaser disk, 90° from the rotation axis). *Left*: In the case of NGC 1194 and NGC 4388 we simply use the large-scale PA of the galaxy. The filled histograms indicate the literature megamasers, where we use the difference in projected position angle between known CO disks in NGC 1068 (Schinnerer et al. 2000), Circinus (Curran et al. 1998), and NGC 3079 (Kondratko et al. 2005). Thus, these measurements are not strictly comparable (ours probes recent star formation while the other directly probes molecular gas). *Right*: In this case the filled histograms include NGC 4258 as well.

serve. Third, the timescales for these warps to operate may be long compared with typical lifetimes.

Changes in angular momentum as a function of scale result naturally in accretion events. Hopkins & Quataert (2010) study the progression of gas from galaxy-wide to pc scales. Because the gas is dissipational, the kinematics of the gas and stars decouple. As a result, the stars are able to torque the gas, leading to warps and ultimately shifts in the angular momentum vector of the gas as a function of scale. Observations of the gas kinematics on $\sim$ 100 pc scales in nearby active galaxies reveal that fueling is indeed facilitated by decoupled dynamical components such as inner bars, ovals or spirals (e.g., Hunt et al. 2008; García-Burillo et al. 2009), but that these fueling episodes are stochastic and short-lived (e.g., Dumas et al. 2007; Haan et al. 2009), in keeping with the observed kinematic misalignment on all spatial scales that we can probe.

In the Hopkins & Quataert models a massive bulge component will suppress these torques, thus requiring different feeding mechanisms (e.g., merging) in bulge-dominated systems (see also their analytic model in Hopkins & Quataert 2011). It is intriguing to note that the megamaser aligns with the large-scale disk in the two bulge-dominated galaxies NGC 1194 and NGC 2960. Our statistics are obviously quite limited. We can use our strong confirmation that nuclear jets align with the rotation axis of megamaser disks (and by extension sub-pc scale disks in general). We look for morphology-dependent alignment in the Kinney et al. (2000) Seyfert sample, with morphological types from the RC3. There is no preference for jet alignment with the rotation axis of the kpc-scale galaxy disk among S0 or S0/a galaxies. However, it would be interesting to investigate possible jet alignment with the rotation axes of circumnuclear $\sim$ 500 pc-scale structures in the Kinney et al. sample (e.g., using *HST*).

Disk misalignments boost accretion rate. Nixon et al. (2012) show that if there are strong misalignments between inner and outer disks, then the gas angular momentum is dissipated where the disks meet, facilitating accretion. As a result, *if* there is a major misalignment as a function of scale, then the accretion rate onto the BH can be boosted by an order of magnitude. We may preferentially observe AGN activity at times of misalignment. With a much larger sample, we could look for an anti-correlation between AGN luminosity and PA alignment as predicted by this model.

The gas has an external origin, and thus knows nothing about the angular momentum of the disk. It would be very challenging to completely rule out that the gas is supplied at random angles via accretion of small satellites. In fact, in the case of NGC 3393 there is tentative evidence for an accretion event in the putative detection of two AGN separated by $\sim$ 150 pc in projection (Fabbiano et al. 2011). Nevertheless, none of the targets shows evidence for morphological disturbance. Given the high incidence of circumnuclear disks and bars in the sample, an internal origin for the accreted gas, with accretion facilitated by secular processes, seems more natural for the bulk of the sample (e.g., Kormendy & Kennicutt 2004).

5. SUMMARY

Using *HST*/WFC3 observations of megamaser disk galaxies, we have shown that the majority of the megamaser disk galaxies contain clear evidence for circumnuclear structures (disks or bars) often with associated star formation. We find that the accretion disk on sub-pc scales (as traced by the megamaser disks) shows no strong tendency to align with circumnuclear (often star-forming) structures such as bars, spirals, or rings on $<$ 500 pc scales. In contrast, we find that the rotation axis of the megamaser disk is usually aligned with the compact radio jet axis. We review possible explanations for the misalignment between circumnuclear and sub-pc scale disks, and favor a scenario in which accretion naturally requires changes in angular momentum as a function of scale. Given the good correlation between the jet and megamaser rotation axis, in the future we can boost the sample statistics using *HST* observations of Seyfert galaxies with radio jets. Furthermore, future direct observations of circumnuclear gas in the megamaser disk galaxies (e.g., with ALMA) will help clarify the processes that feed the central monster.

We would like to thank Paul Martini, Jeremy Goodman, Eliot

Quataert, Jim Ulvestad, and John Kormendy for very useful conversations. We thank the anonymous referee for a timely and thorough report that improved this manuscript.

REFERENCES

Ann, H. B., & Thakur, P. 2005, ApJ, 620, 197
Balick, B., & Heckman, T. M. 1982, ARA&A, 20, 431
Barbosa, F. K. B., Storchi-Bergmann, T., Cid Fernandes, R., Winge, C., & Schmitt, H. 2006, MNRAS, 371, 170
Braatz, J. A., Wilson, A. S., & Henkel, C. 1997, ApJS, 110, 321
Bregman, M., & Alexander, T. 2012, ApJ, 748, 63
Bressan, A., Marigo, P., Girardi, L., Salasnich, B., Dal Cero, C., Rubele, S., & Nanni, A. 2012, MNRAS, 427, 127
Buta, R. 1986, ApJS, 61, 609
Buta, R., & Crocker, D. A. 1993, AJ, 105, 1344
Cooke, A. J., Baldwin, J. A., Ferland, G. J., Netzer, H., & Wilson, A. S. 2000, ApJS, 129, 517
Curran, S. J., Johansson, L. E. B., Rydbeck, G., & Booth, R. S. 1998, A&A, 338, 863
Davies, R. I., Maciejewski, W., Hicks, E. K. S., Tacconi, L. J., Genzel, R., & Engel, H. 2009, ApJ, 702, 114
Dumas, G., Mundell, C. G., Emsellem, E., & Nagar, N. M. 2007, MNRAS, 379, 1249
Duric, N., & Seaquist, E. R. 1988, ApJ, 326, 574
Englmaier, P., & Shlosman, I. 2000, ApJ, 528, 677
Erwin, P., & Sparke, L. S. 2003, ApJS, 146, 299
Fabbiano, G., Wang, J., Elvis, M., & Risaliti, G. 2011, Nature, 477, 431
Falcke, H., Wilson, A. S., & Simpson, C. 1998, ApJ, 502, 199
Falcón-Barroso, J., et al. 2006, MNRAS, 369, 529
Gammie, C. F., Goodman, J., & Ogilvie, G. I. 2000, MNRAS, 318, 1005
García-Burillo, S., et al. 2009, A&A, 496, 85
Girardi, L., et al. 2008, PASP, 120, 583
Greene, J. E., et al. 2010, ApJ, 721, 26
Greenhill, L. J., Kondratko, P. T., Moran, J. M., & Tilak, A. 2009, ApJ, 707, 787
Greenhill, L. J., et al. 2003, ApJ, 590, 162
Haan, S., Schinnerer, E., Emsellem, E., García-Burillo, S., Combes, F., Mundell, C. G., & Rix, H.-W. 2009, ApJ, 692, 1623
Henkel, C., Peck, A. B., Tarchi, A., Nagar, N. M., Braatz, J. A., Castangia, P., & Moscadelli, L. 2005, A&A, 436, 75
Herrnstein, J. R., Moran, J. M., Greenhill, L. J., Diamond, P. J., Inoue, M., Nakai, N., Miyoshi, M., Henkel, C., & Riess, A. 1999, Nature, 400, 539
Hopkins, P. F., Hernquist, L., Cox, T. J., Di Matteo, T., Robertson, B., & Springel, V. 2006, ApJS, 163, 1
Hopkins, P. F., & Quataert, E. 2010, MNRAS, 407, 1529
—. 2011, MNRAS, 415, 1027
Hunt, L. K., et al. 2008, A&A, 482, 133
Impellizzeri, C. M. V., Braatz, J. A., Kuo, C.-Y., Reid, M. J., Lo, K. Y., Henkel, C., & Condon, J. J. 2012, in IAU Symposium, Vol. 287, IAU Symposium, ed. R. S. Booth, W. H. T. Vlemmings, & E. M. L. Humphreys, 311–315
Ishihara, Y., Nakai, N., Iyomoto, N., Makishima, K., Diamond, P., & Hall, P. 2001, PASJ, 53, 215
Jedrzejewski, R. I. 1987, MNRAS, 226, 747
Kartje, J. F., Königl, A., & Elitzur, M. 1999, ApJ, 513, 180
Kim, W.-T., Seo, W.-Y., Stone, J. M., Yoon, D., & Teuben, P. J. 2012, ApJ, 747, 60
Kinney, A. L., Schmitt, H. R., Clarke, C. J., Pringle, J. E., Ulvestad, J. S., & Antonucci, R. R. J. 2000, ApJ, 537, 152
Koda, J., et al. 2002, ApJ, 573, 105
Kondratko, P. T., Greenhill, L. J., & Moran, J. M. 2005, ApJ, 618, 618
—. 2008, ApJ, 678, 87
Kormendy, J., & Kennicutt, Jr., R. C. 2004, ARA&A, 42, 603
Kuo, C., Braatz, J. A., Reid, M. J., Lo, F. K. Y., Condon, J. J., Impellizzeri, C. M. V., & Henkel, C. 2013, ApJ, 767, 155
Kuo, C. Y., et al. 2011, ApJ, 727, 20
Li, Z.-Y., Ho, L. C., Barth, A. J., & Peng, C. Y. 2011, ApJS, 197, 22
Lo, K. Y. 2005, ARA&A, 43, 625
Maciejewski, W. 2004, MNRAS, 354, 892
Maciejewski, W., Teuben, P. J., Sparke, L. S., & Stone, J. M. 2002, MNRAS, 329, 502
Maloney, P. R., Begelman, M. C., & Pringle, J. E. 1996, ApJ, 472, 582
Martini, P., Regan, M. W., Mulchaey, J. S., & Pogge, R. W. 2003, ApJ, 589, 774
McKinney, J. C., Tchekhovskoy, A., & Blandford, R. D. 2013, Science, 339, 49
Menéndez-Delmestre, K., Sheth, K., Schinnerer, E., Jarrett, T. H., & Scoville, N. Z. 2007, ApJ, 657, 790
Middelberg, E., et al. 2004, A&A, 417, 925
Miyoshi, M., Moran, J., Herrnstein, J., Greenhill, L., Nakai, N., Diamond, P., & Inoue, M. 1995, Nature, 373, 127
Morganti, R., Tsvetanov, Z. I., Gallimore, J., & Allen, M. G. 1999, A&AS, 137, 457
Nixon, C., King, A., & Price, D. 2012, MNRAS, accepted (arXiv:1203.0008)
Petitpas, G. R., & Wilson, C. D. 2002, ApJ, 575, 814
Pogge, R. W., & Martini, P. 2002, ApJ, 569, 624
Pringle, J. E. 1997, MNRAS, 292, 136
Pringle, J. E., Antonucci, R. R. J., Clarke, C. J., Kinney, A. L., Schmitt, H. R., & Ulvestad, J. S. 1999, ApJ, 526, L9
Reid, M. J., Braatz, J. A., Condon, J. J., Greenhill, L. J., Henkel, C., & Lo, K. Y. 2009, ApJ, 695, 287
Reid, M. J., Braatz, J. A., Condon, J. J., Lo, K. Y., Kuo, C. Y., Impellizzeri, C. M. V., & Henkel, C. 2013, ApJ, 767, 154
Sanders, D. B., Soifer, B. T., Elias, J. H., Neugebauer, G., & Matthews, K. 1988, ApJ, 328, L35
Schinnerer, E., Eckart, A., Tacconi, L. J., Genzel, R., & Downes, D. 2000, ApJ, 533, 850
Schmitt, H. R., Ulvestad, J. S., Antonucci, R. R. J., & Kinney, A. L. 2001, ApJS, 132, 199
Shlosman, I., Begelman, M. C., & Frank, J. 1990, Nature, 345, 679
Storchi-Bergmann, T., Dors, Jr., O. L., Riffel, R. A., Fathi, K., Axon, D. J., Robinson, A., Marconi, A., & Östlin, G. 2007, ApJ, 670, 959
Trotter, A. S., Greenhill, L. J., Moran, J. M., Reid, M. J., Irwin, J. A. & Lo, K.-Y. 1998, ApJ, 495, 740
Ulvestad, J. S., Roy, A. L., Colbert, E. J. M., & Wilson, A. S. 1998, ApJ, 496, 196
Ulvestad, J. S., & Wilson, A. S. 1984, ApJ, 285, 439
Wozniak, H., Friedli, D., Martinet, L., Martin, P., & Bratschi, P. 1995, A&AS, 111, 115